

Core polarization in coupled-cluster theory induced by a parity and time-reversal violating interaction

K.V.P. Latha ^{*}, Dilip Angom [†], Rajat K.Chaudhuri ^{*}, B.P. Das^{*} and

Debashis Mukherjee ^{**}

^{*} *Indian Institute of Astrophysics, Koramangala, Bangalore, Karnataka, INDIA - 560 034.*

[†] *Physical Research Laboratory, Navarangapura, Ahmedabad, Gujarat, INDIA - 380009. and*

^{**} *Indian Association of Cultivation of Science,*

Kolkata, West Bengal, INDIA - 700032.

Email: latha@iiap.res.in

(Dated: February 5, 2008)

The effects of parity and time reversal violating potential, in particular the tensor-pseudotensor electron nucleus interaction are studied. We establish that selected terms representing the interplay of these effects and the residual Coulomb interaction in the coupled-cluster method are equivalent to the coupled perturbed Hartree-Fock. We have shown that the *normal* CPHF diagrams have a one-one correspondance in the coupled-cluster theory, but the CPHF pseudo diagrams are present in a subtle way. We have studied the *pseudo* diagrams in great detail and have shown explicitly their origin in coupled-cluster theory. This is demonstrated by considering the case of the permanent electric dipole moment of atomic Hg and our results are compared with the results of an earlier calculation.

PACS numbers: 32.10.Dk,11.30.Er,31.15.Dv

I. INTRODUCTION

The observation of a non-zero intrinsic electric dipole moment (EDM) of a non-degenerate quantum system is an evidence of parity (P) and time-reversal (T) symmetry violations [1, 2]. Among the two, T violation is of particular interest as it is less understood and has important implications for physics beyond the standard model. In the experiments where CP violation has been observed so far [3, 4, 5], T violation is inferred [6] by invoking the CPT theorem. However, the observation of an EDM would be a direct evidence of T violation in nature. Atoms are suitable and promising candidates to measure permanent EDMs due to their sensitivity to the P and T violating phenomena in the nuclear (hadronic), electron-nucleus (semi-leptonic) and electron (leptonic) sectors [7]. In this paper, we study the atomic EDM arising from the tensor-pseudotensor electron-nucleus interactions, which is semileptonic in nature. The coupling constant C_T of this interaction is zero within the standard model but it is finite in some theories which are extensions of the standard model [8]. The closed shell atoms are sensitive to this interaction due to its dependence on the nuclear spin and heavier atoms are more sensitive to this interaction since it scales as Z^2 [9]. The closed shell atoms on which EDM experiments have been performed to date are ^{199}Hg [10] and ^{129}Xe [11, 12, 13] and efforts are underway to improve the results. In addition, new experiments are planned for Yb [14, 15] and Ra [16]. The ^{199}Hg experimental data has been used to provide improved limits on important P,T odd coupling constants at the elementary particle level [10]. These have been extracted by combining atomic calculations [17] and experiments [10]. The coupled-perturbed Hartree Fock (CPHF) [18] effects are extremely important in the calculation of atomic proper-

ties and it is particularly true in the case of the atomic EDMs [19]. It is important to analyze these effects in the framework of an all-order many-body method like the coupled-cluster method [20], one of the most accurate many-body methods for the study of atomic properties [21]. The main thrust of this work is to demonstrate that all the CPHF effects are subsumed in the coupled-cluster method. This is an important step towards improving the accuracy of the existing atomic calculations of closed-shell atomic EDMs, which is necessary for obtaining better limits on the P and T violating coupling constants. A similar study has been done for parity non-conservation effects in open shell atoms [22]. This paper is organized as follows : In Section II we present the theoretical background, in Section III, we discuss the coupled-cluster equations with/without the T-PT interaction, in Section IV we discuss the atomic EDM in the coupled-cluster and the CPHF framework, in Section V we discuss our results and finally we present our conclusions in Section VI.

II. THEORETICAL BACKGROUND

A. Dirac-Fock equation

For heavy atoms, the relativistic effects cannot be neglected and should be incorporated in the atomic Hamiltonian. An approximate relativistic atomic Hamiltonian, appropriate for our calculations is the Dirac-Coulomb Hamiltonian H_{DC} . For an N electron atomic system in atomic units

$$H_{\text{DC}} = \sum_i^N [c\boldsymbol{\alpha}_i \cdot \mathbf{p}_i + \beta_i c^2 + V_N(\vec{r}_i)] + \sum_{i<j}^N \frac{1}{r_{ij}}, \quad (1)$$

where c is velocity of light, α and β are the Dirac matrices and \vec{r}_{ij} is the separation between the i th and j th electrons. This Hamiltonian is an approximation to the general atomic Hamiltonian, which consists of additional terms arising from the interaction of electron spin with nuclear spin, interaction between spins of electrons, magnetic interactions, etc. However, these interactions are neglected as their strength is negligible compared to the electron-electron Coulomb interaction and the nuclear potential energy.

The single electron equations are obtained by approximating the two-electron Coulomb interaction by the Dirac-Fock central potential $U_{\text{DF}}(\vec{r}_i)$. Then

$$H_{\text{DC}} = \sum_i^N [c\alpha_i \cdot \mathbf{p}_i + \beta_i c^2 + V_N(\vec{r}_i) + U_{\text{DF}}(\vec{r}_i)] + V_{\text{es}}, \quad (2)$$

where the residual Coulomb interaction

$$V_{\text{es}} = \sum_{i,j,i < j} \frac{1}{\vec{r}_{ij}} - \sum_i U_{\text{DF}}(\vec{r}_i).$$

The residual Coulomb interaction embodies the non-central or correlation effects, which can be incorporated in the atomic theory calculations as a perturbation. The single electron wavefunctions satisfy the Schroedinger equation

$$[c\alpha \cdot \mathbf{p} + \beta c^2 + V_N(\vec{r}) + U_{\text{DF}}(\vec{r})] |\psi_a^0\rangle = \epsilon_a^0 |\psi_a^0\rangle, \quad (3)$$

where $|\psi_a^0\rangle$ is the single electron wavefunction and a denotes the quantum numbers which specify the wavefunction uniquely and ϵ_a^0 are the single electron energies. We can group the operators in the equation and rewrite the equation as

$$(t + g^0 - \epsilon_a^0) |\psi_a^0\rangle = 0. \quad (4)$$

In the above equation $t = c\alpha \cdot \mathbf{p} + \beta c^2 + V_N(\vec{r})$ and the Dirac-Fock potential $g^0 |\psi_a^0\rangle = \sum_{b=1}^{N_{\text{occ}}} [\langle \psi_b^0 | v | \psi_b^0 \rangle |\psi_a^0\rangle - \langle \psi_b^0 | v | \psi_a^0 \rangle |\psi_b^0\rangle]$, here $v = 1/(\vec{r}_1 - \vec{r}_2)$, \vec{r}_i being the position coordinate of the i th electron and the summation is over all the occupied orbitals in the reference state. If an atom has a non-zero EDM, then it is an indication of P and T violating interactions within the atom. In this paper, we consider the atomic EDM arising from the tensor-pseudo tensor P and T violating electron-nuclear interaction

$$H_{\text{T-PT}} = i 2\sqrt{2} C_T G_F \beta \alpha \cdot \mathbf{I} \rho(\vec{r}), \quad (5)$$

where G_F and $\rho(\vec{r})$ are the Fermi coupling constant and nuclear density respectively, β and α are the Dirac matrices and \mathbf{I} is the nuclear spin. This interaction perturbs g^0 and the orbitals acquire an admixture from the opposite parity orbitals. At the single electron level, these effects are incorporated in the CPHF calculations.

B. Coupled-perturbed Hartree-Fock

The introduction of the P and T violating interaction, $h_{\text{T-PT}}$, as a perturbation modifies the atomic Hamiltonian. The corresponding single electron wavefunctions are the mixed parity states

$$|\tilde{\psi}_a\rangle = |\psi_a^0\rangle + \lambda |\psi_a^1\rangle, \quad (6)$$

where λ is the perturbation parameter and $|\psi_a^1\rangle$ is the first order correction, which is opposite in parity to $|\psi_a^0\rangle$. However, there is no first order energy correction as $h_{\text{T-PT}}$ is parity odd. Then the perturbed Dirac-Fock equation is

$$\left[h^0 + \lambda h_{\text{T-PT}} + \sum_{b=1}^{N_{\text{occ}}} \langle \tilde{\psi}_b | v | \tilde{\psi}_b \rangle - \epsilon_a^0 \right] |\tilde{\psi}_a\rangle - \sum_{b=1}^{N_{\text{occ}}} \langle \tilde{\psi}_b | v | \tilde{\psi}_a \rangle |\tilde{\psi}_b\rangle = 0. \quad (7)$$

Selecting terms linear in λ and rearranging we get the CPHF equation

$$(h^0 + g^0 - \epsilon_a^0) |\psi_a^1\rangle = (-h_{\text{T-PT}} - g^1) |\psi_a^0\rangle. \quad (8)$$

The perturbed Dirac-Fock operator

$$g^1 |\psi_a^0\rangle = \sum_{b=1}^{N_{\text{occ}}} [\langle \psi_b^0 | v | \psi_b^1 \rangle |\psi_a^0\rangle - \langle \psi_b^0 | v | \psi_a^0 \rangle |\psi_b^1\rangle + \langle \psi_b^1 | v | \psi_b^0 \rangle |\psi_a^0\rangle - \langle \psi_b^1 | v | \psi_a^0 \rangle |\psi_b^0\rangle]. \quad (9)$$

In the present work, to solve Eq.(8), we expand $|\psi_a^1\rangle$ in terms of a complete set of unperturbed opposite parity orbitals. Then, $|\psi_a^1\rangle = \sum_p C_{pa} |\psi_p^0\rangle$, where C_{pa} are the mixing coefficients. Substituting this in Eq.(8) and projecting by $\langle \psi_p^0 |$, we obtain a set of linear algebraic equations

$$C_{pa} (\epsilon_p^0 - \epsilon_a^0) + \sum_{bq} \left[\tilde{V}_{pqab} C_{qb}^* + \tilde{V}_{pbaq} C_{qb} \right] + \langle p | h_{\text{T-PT}} | a \rangle = 0, \quad (10)$$

where $\tilde{V}_{pqab} = \langle pq | v | ab \rangle - \langle pq | v | ba \rangle$ and $\tilde{V}_{pbaq} = \langle pb | v | aq \rangle - \langle pb | v | qa \rangle$. Another approach to calculate $|\psi_a^1\rangle$ is to solve Eq.(8) self-consistently [17]. Hereafter, for brevity, an orbital $|\psi_i\rangle$ is represented as $|i\rangle$. Eq.(10) can be written as the matrix equation

$$AC = -B, \quad (11)$$

where $A_{pa} = \sum_{bq} (\tilde{V}_{pqab} + \tilde{V}_{pbaq} + (\epsilon_p^0 - \epsilon_a^0) \delta_{pq} \delta_{ab})$ and $B_{pa} = \langle p | h_{\text{T-PT}} | a \rangle$. This equation is solved iteratively starting with the zeroth order (in v) contribution

$$C_{pa}^{(0,1)} = -\frac{B_{pa}}{\epsilon_p^0 - \epsilon_a^0} \quad (12)$$

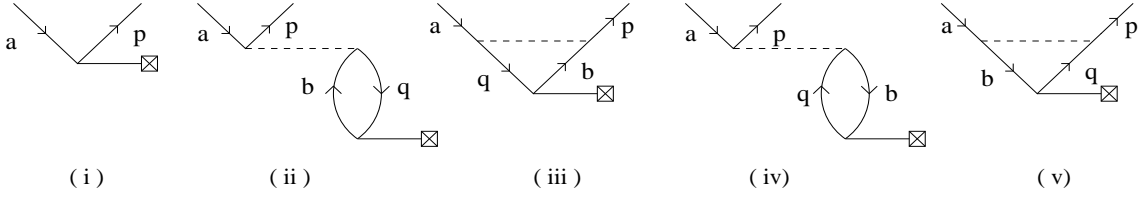


FIG. 1: CPHF diagrams at zero and one order Coulomb interaction, v . The diagrams (ii,iii) are the *pseudo* CPHF diagrams and (iv,v) are the *normal* CPHF diagrams. The dotted line is the Coulomb interaction and the line attached with \boxtimes is the T-PT interaction. Pseudo diagrams are the diagrams with local energy denominators, note the direction of b and q orbitals.

as the initial guess. The coefficients in the k^{th} iteration are

$$C_{pa}^{(k,1)} = \frac{-B_{pa} - \sum_{bq} \left(\tilde{V}_{pqab} C_{qb}^{(k-1,1)*} + \tilde{V}_{pbaq} C_{qb}^{(k-1,1)} \right)}{\epsilon_p^0 - \epsilon_a^0}. \quad (13)$$

The superscripts in $C_{pa}^{(k,1)}$ refer to the order of v and $h_{\text{T-PT}}$ respectively. The diagrams arising from the above equation in zero and one order of v are shown in Fig.1. In this paper, the diagrams of the second and the third terms in Eq.(13) are referred to as the *pseudo* and *normal* diagrams respectively.

III. COUPLED-CLUSTER EQUATIONS

In the coupled cluster theory, the exact atomic state

$$|\Psi\rangle = e^{T^{(0)}} |\Phi_0\rangle, \quad (14)$$

where $T^{(0)}$ is the cluster operator and $|\Phi_0\rangle$ is the reference state. For the ground state, $|\Phi_0\rangle$ is the Slater-determinant of all the occupied orbitals. The cluster operator $T^{(0)} = \sum_i T_i^{(0)}$, where $T_i^{(0)}$ are the i -tuple excitation operators. The cluster amplitude equations are obtained from, after applying the operator $e^{-T^{(0)}}$ and projecting on excited states, the Schroedinger equation of $|\Psi\rangle$. Restricting to the approximation $T^{(0)} = T_1^{(0)} + T_2^{(0)}$, the cluster operators are hence solutions of the equation $\langle \Phi^* | \bar{H}_N | \Phi_0 \rangle = 0$, where $|\Phi^*\rangle$ denotes singly and doubly excited states $|\Phi_a^r\rangle$ and $|\Phi_{ab}^s\rangle$ respectively. For any operator O , $\bar{O} = e^{-T^{(0)}} O e^{T^{(0)}}$ is the dressed operator. It is to be noted that H_N is the normal ordered atomic Hamiltonian, which is H_{DC} in the present calculations. Let the $H_{\text{T-PT}}$ perturbed atomic state

$$|\Psi'\rangle = e^{T^{(0)} + \lambda T^{(1)}} |\Phi_0\rangle, \quad (15)$$

where $T^{(1)}$ is the $H_{\text{T-PT}}$ perturbed cluster operator and λ as defined earlier, is the perturbation parameter. The perturbed coupled cluster equations are

$$\langle \Phi^{*'} | [\bar{H}_N, T^{(1)}] | \Phi_0 \rangle = -\langle \Phi^{*'} | \bar{H}_N^{\text{T-PT}} | \Phi_0 \rangle, \quad (16)$$

where $|\Phi^{*'}\rangle$ are opposite in parity to $|\Phi_0\rangle$ and $\bar{H}_N^{\text{T-PT}}$ is the normal ordered dressed $H_{\text{T-PT}}$. Defining $\{O_1 O_2\}$

as the *contraction* and normal order of two operators O_1 and O_2 , then

$$[\bar{H}_N, T^{(1)}] = \overline{\{\bar{H}_N T^{(1)}\}}. \quad (17)$$

Consider $T^{(1)} = T_1^{(1)}$, the singles equation from Eq.(16) is

$$\langle \Phi_a^{p'} | \overline{\{\bar{H}_N T_1^{(1)}\}} | \Phi_0 \rangle = -\langle \Phi_a^{p'} | \bar{H}_N^{\text{T-PT}} | \Phi_0 \rangle. \quad (18)$$

The cluster operator $T_1^{(1)} = \sum_{a,p} a_p^\dagger a_a t_a^p$ and t_a^p is the associated cluster amplitude. Retaining only $H_N^{\text{T-PT}}$ from $\bar{H}_N^{\text{T-PT}}$, in terms of matrix elements

$$\sum_{bq} \tilde{V}_{pb\ aq} t_b^{q(1)} + (\epsilon_p^{(0)} - \epsilon_a^{(0)}) t_a^{p(1)} = -B_{pa}. \quad (19)$$

Then the perturbed cluster amplitudes $t_a^{p(1)}$, are solutions of the iterative equation

$$t_a^{p(k,1)} = \frac{-B_{pa} - \sum_{bq} \tilde{V}_{pb\ aq} t_b^{q(k-1,1)}}{\epsilon_p^{(0)} - \epsilon_a^{(0)}}. \quad (20)$$

This is equivalent to the Eq.(13), the equation of the CPHF mixing coefficients without the *pseudo* diagrams. This formally establishes that the *normal* diagrams in the CPHF approach are equivalent to a subset of terms in the coupled-cluster theory. However, a similar comparison of the *pseudo* diagrams in the CPHF and the coupled-cluster theories is done later as it requires the dressed electric dipole operator \bar{D} , defined in the next section through the atomic EDM.

IV. ATOMIC EDM

A. General expression

The atomic EDM in the CPHF approximation is

$$\begin{aligned} D_a &= \sum_{ap} \langle a|d|p\rangle C_{pa}^{(\infty,1)} + C_{pa}^{*(\infty,1)} \langle p|d|a\rangle, \\ &= 2 \sum_{ap} \langle a|d|p\rangle C_{pa}^{(\infty,1)}, \end{aligned} \quad (21)$$

where d is the single particle electric dipole operator and the first superscript on the mixing coefficients refers to all order in v . The diagrams which contribute to D_a are shown in Fig.2. The mixing coefficients in Eq.(13) has v to all orders in the limit $k \rightarrow \infty$. Substituting the expression of $C_{pa}^{(\infty,1)}$, we have

$$D_a = -2 \sum_{ap} \frac{\langle a|d|p\rangle}{\epsilon_p^0 - \epsilon_a^0} \left[B_{pa} + \sum_{bq} \left(\tilde{V}_{pqab} C_{qb}^{(k-1,1)*} + \tilde{V}_{pbqa} C_{qb}^{(k-1,1)} \right) \right]. \quad (22)$$

In coupled-cluster theory, the atomic EDM

$$D_a = \langle \Phi_0 | T^{(1)\dagger} \bar{D} + \bar{D} T^{(1)} | \Phi_0 \rangle. \quad (23)$$

It should be noted that D_a has linked terms only [23], the unlinked terms cancels the normalization factor. For the *normal* diagrams, the two terms in Eq.(23) are equivalent and arise from $D(T_{1\text{eff}}^{(1)})$. Here $T_{1\text{eff}}^{(1)}$ is the contraction of $T_1^{(1)}$ with v -see Fig.1(iv),(v).

B. Pseudo diagrams

The diagrams in the Fig.2 (ii) and (iii) are the sum of two many-body perturbation theory diagrams. We now show that, in coupled-cluster theory these are subsumed in $D_a = \langle \Phi_0 | [DT_{1\text{eff}}^{(1)} + T_1^{(1)\dagger} DT_2^{(0)}] | \Phi_0 \rangle$. Unlike in *normal* terms, here, $T_{1\text{eff}}^{(1)} = H_{T-PT} T_2^{(0)}$. The operator $T_2^{(0)}$ has correlation effects arising from the two-particle and two-hole as well as the other forms of v , to all orders. Hence, the CPHF *pseudo* diagrams do not have a one-one correspondence with the above CCEDM terms, rather the *pseudo* diagrams are part of terms in CCEDM.

The algebraic expressions of the EDM diagrams shown in Fig. 2 (ii,iii) are,

$$\frac{\langle a|D|p\rangle \langle pq|v|ab\rangle \langle b|h_{T-PT}|q\rangle}{(\epsilon_p - \epsilon_a)(\epsilon_b - \epsilon_q)}, \quad (24)$$

and

$$\frac{\langle a|D|p\rangle \langle pq|v|ba\rangle \langle b|h_{T-PT}|q\rangle}{(\epsilon_p - \epsilon_a)(\epsilon_b - \epsilon_q)}, \quad (25)$$

respectively. The diagram in Fig .2(ii) is the sum of the two MBPT diagrams topologically equivalent to Fig. 3-I(a) and I(b), algebraically

$$\frac{\langle a|D|p\rangle \langle pq|v|ab\rangle \langle b|h_{T-PT}|q\rangle}{\epsilon_a + \epsilon_b - \epsilon_p - \epsilon_q} \left[\frac{1}{\epsilon_a - \epsilon_p} + \frac{1}{\epsilon_b - \epsilon_q} \right]. \quad (26)$$

On simplification, this is same as Eq. (24) multiplied by a phase (-1). Similarly, the exchange diagram Fig. 2(iii) is

the sum of the topologically equivalent MBPT diagrams of Fig.3 II (a) and (b), algebraically

$$\frac{\langle a|D|p\rangle \langle pq|v|ba\rangle \langle b|h_{EDM}|q\rangle}{\epsilon_a + \epsilon_b - \epsilon_p - \epsilon_q} \left[\frac{1}{\epsilon_a - \epsilon_p} + \frac{1}{\epsilon_b - \epsilon_q} \right], \quad (27)$$

which is equivalent to Eq. 25, apart from a phase = (-1). To calculate the cluster amplitudes which has similar correlation effects, retain H_{T-PT} and $\overline{H_{T-PT} T_2^{(0)}}$ in Eq. (18). Then cluster amplitude equation is

$$T_a^{p(k,1)} = \frac{-B'_{ap} - \sum_{bq} \tilde{V}_{pbqa} t_a^{(k-1,1)}}{\epsilon_p - \epsilon_a}. \quad (28)$$

where $B'_{ap} = (H_{T-PT} + \overline{H_{T-PT} T_2^{(0)}})_{ap}$. The cluster amplitudes calculated from the above equation has effects of direct and exchange *pseudo* diagrams.

To analyse the atomic EDM arising from the *pseudo* diagrams within the coupled-cluster theory, consider the two terms $DT_{1\text{eff}}^{(1)}$ and $T_1^{(1)\dagger} DT_2^{(0)}$. After introducing complete set of eigen functions, the contribution to D_a from these terms

$$D_a = \sum_I \left[\langle \Phi_0 | D | \Phi_I \rangle \langle \Phi_I | T_1^{(1)} | \Phi_0 \rangle + \sum_J \langle \Phi_0 | T_1^{(1)\dagger} | \Phi_I \rangle \langle \Phi_I | D | \Phi_J \rangle \langle \Phi_J | T_2^{(0)} | \Phi_0 \rangle \right] \quad (29)$$

The first term on the right hand side, in terms of determinantal states, the contribution to the *pseudo* diagram is

$$\sum_{a,p} \langle \Phi_0 | D | \Phi_a^p \rangle \langle \Phi_a^p | (T_1^{(1)})_{\text{eff}} | \Phi_0 \rangle, \quad (30)$$

this follows as D and $T_1^{(1)}$ are single particle operators. It is to be mentioned that, the $(T_1^{(1)})_{\text{eff}}$ represents the component of $T_1^{(1)}$ arising from the term $\overline{(H_{T-PT} T_2^{(0)})_{ap}}$ in Eq.(28). Similarly, the second term in Eq.(29) is

$$\sum_{ap,bq} \langle \Phi_0 | T_1^{(1)\dagger} | \Phi_a^p \rangle \langle \Phi_a^p | D | \Phi_{ab}^{pq} \rangle \langle \Phi_{ab}^{pq} | T_2^{(0)} | \Phi_0 \rangle. \quad (31)$$

In this expression, the *pseudo* diagram contributions are present in the component of $T_1^{(1)}$ arising from the term $(H_{T-PT})_{ap}$ in Eq.(28). Using Slater-Condon rules, the matrix elements of single and two-particle operators between determinantal states are: $\langle \Phi_a^p | D | \Phi_0 \rangle = \langle p | D | a \rangle$; $\langle \Phi_{ab}^{pq} | T_2^{(0)} | \Phi_0 \rangle = \langle pq | t_2 | ab \rangle - \langle pq | t_2 | ba \rangle$ and $\langle \Phi_a^p | D | \Phi_{ab}^{pq} \rangle = \langle b | D | q \rangle$. Then,

$$D_a = \sum_{a,p} \langle p | D | a \rangle \langle a | (T_1^{(1)})_{\text{eff}} | p \rangle + \sum_{ap,bq} t_{bq}^{(1)\dagger} \langle a | D | p \rangle [\langle pq | t_2 | ab \rangle - \langle pq | t_2 | ba \rangle] \quad (32)$$

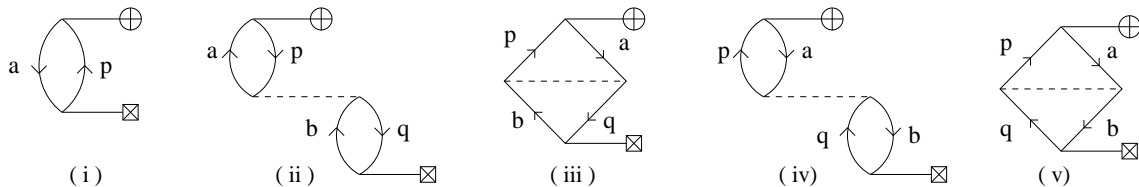


FIG. 2: CPHF diagrams contributing to EDM. (ii,iii) and (iv,v) are the EDM diagrams arising from *pseudo* and the *normal* CPHF diagrams respectively. The lines with \oplus denote *dipole* operator. When V_{es} is treated to all orders, the EDM interaction vertex is equivalent to the mixing coefficients in CPHF and singles cluster amplitude in CC.

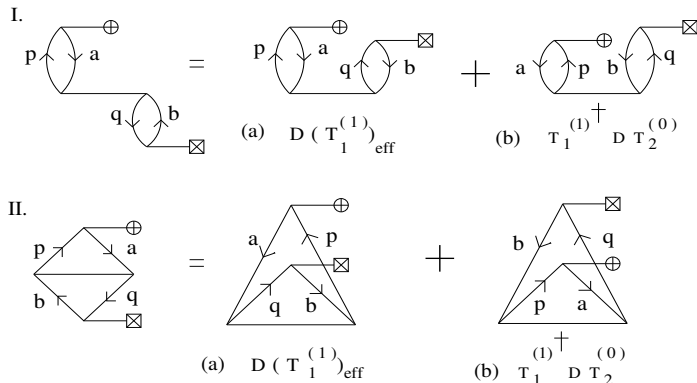


FIG. 3: Diagrams contributing to EDM - Solid interaction lines in I(a)&(b), II(a)&(b) and III(a)&(b) represent the Coulomb interaction treated to all orders. The operator $T_1^{(1)}{}_{\text{eff}}$ is a result of the contraction $T_2^{(0)}T_1^{(1)\dagger}$, which, when contracted with the induced dipole operator (D), gives the diagram contributing to D_a .

The effects of the *pseudo* diagrams are distributed among various terms with the $T_2^{(0)}$ cluster amplitude. Hence, it is difficult to establish one-one correspondence between the CPHF pseudo diagrams and the corresponding diagrams in CCEDM in orders of v . This is a consequence of the structure of CCEDM and CPHF equations where the perturbed cluster amplitudes are computed using the converged values of the $T_2^{(0)}$ amplitudes, which treat the residual coulomb interaction to all orders. However, the converged results which includes all orders of v and one order of H_{T-PT} , where the sequence of the perturbations has all possible combinations, should be identical. It is possible to establish the equivalence by choosing only the two-particle two-hole terms of v in the $T_2^{(0)}$ equations.

In this paper, we calculate the *normal* and the *pseudo* diagrams simultaneously, this couples the *normal* and *pseudo* contributions. This is evident from the Eq. (13), where the CPHF coefficients are iterated with both the *normal* and the *pseudo* diagrams. But within the coupled-cluster theory, in particular CCEDM formalism, this inclusion is more subtle. This is due to the structure of Eq. (23), where the converged $T^{(1)}$ amplitudes contain the effects of the EDM from both the terms shown in Eq. (28).

V. RESULTS

A. Symmetrywise contribution

From the expression of H_{T-PT} , the presence of nuclear density $\rho(r)$, $s_{1/2} - p_{1/2}$ is expected to have the largest contribution. This is indeed observed in our calculations. The variation of D_a for a small basis consisting of 68 Gaussian type orbitals [24]: (1-12) $s_{1/2}$, (2-13) $p_{1/2,3/2}$, (3-10) $d_{3/2,5/2}$, (4-7) $f_{5/2,7/2}$ and (5-8) $g_{7/2,9/2}$, are given in Table.I. It lists the value of D_a when or-

TABLE I: Variation of D_a with the inclusion of higher angular momentum virtual states. The first column implies that virtuals only upto the orbitals indicated have been included in the calculation, in addition to $s_{1/2}$ and $p_{1/2}$ symmetries. The *normal* and the two *pseudo* diagrams are calculated independently.

Virtual states	EDM ($\times 10^{-22}$ e-m)	
	Normal	(Normal+Pseudo)
upto $p_{3/2}$	-6.411	-6.024
upto $d_{5/2}$	-6.415	-6.127
upto $f_{7/2}$	-6.399	-6.142
upto $g_{9/2}$	-6.399	-6.144

bitals are added symmetrywise. According to the table D_a , the contribution from the higher angular momentum d and f virtual orbitals are small and opposite in phase. Next, we consider an optimal basis set, with which we get converged D_a , it consists 112 Gaussian type orbitals: (1-18) $s_{1/2}$, (2-18) $p_{1/2,3/2}$, (3-16) $d_{3/2,5/2}$, (4-13) $f_{5/2,7/2}$ and (5-10) $g_{7/2,9/2}$. The results from the optimal basis are

TABLE II: Variation of D_a with the inclusion of higher angular momentum virtual states. The first column implies that virtuals only upto the orbitals indicated have been included in the calculation, in addition to $s_{1/2}$ and $p_{1/2}$ symmetries. The normal and the two *pseudo* diagrams have been calculated together.

Virtual states	EDM ($\times 10^{-22}$ e-m)
upto $p_{3/2}$	-5.83
upto $d_{5/2}$	-5.90
upto $f_{7/2}$	-6.75
upto $g_{9/2}$	-6.75

given in Table.II. It lists D_a arising from the *normal* and

pseudo, where these are calculated simultaneously. It can be seen that the contribution from the virtual orbitals enhances D_a and changes the value $-5.83 \times 10^{-22}em$ to $-6.75 \times 10^{-22}em$.

For a more detailed analysis, the dominant contributions from $6s_{1/2}-p_{1/2}$ and $6s_{1/2}-p_{3/2}$ are listed in Table. III. The total contribution from the $6s_{1/2}-np_{1/2,3/2}$ from

TABLE III: Dominant contributions to $D_a = T_1^{(1)}D + T_1^{(1)}DT_2^{(0)}$ (in units of $10^{-22}C_T em \sigma_N$) from the terms shown in Eq. 28 for np intermediate states calculated using the coupled-cluster theory for EDMs.

Occ.	np	$T_1^{(1)}$	D	D_a $T_1^{(1)}D$
$6s_{1/2}$	$6p_{1/2}$	104.69	0.872	-1.010
$6s_{1/2}$	$7p_{1/2}$	-254.88	-1.821	-5.139
$6s_{1/2}$	$8p_{1/2}$	262.28	1.388	-4.032
$6s_{1/2}$	$9p_{1/2}$	-202.37	-0.344	-0.771
$6s_{1/2}$	$10p_{1/2}$	-113.94	0.068	0.0858
$6s_{1/2}$	$11p_{1/2}$	-56.22	0.692	0.0431
$6s_{1/2}$	$6p_{3/2}$	13.85	0.995	0.153
$6s_{1/2}$	$7p_{3/2}$	-36.27	-2.372	0.953
$6s_{1/2}$	$8p_{3/2}$	-36.80	-2.211	0.901
$6s_{1/2}$	$9p_{3/2}$	15.91	0.771	0.0135
Total				-8.2026

the term $T_1^{(1)\dagger}DT_2^{(0)}$ is $-0.337 \times 10^{-22}C_T em \sigma_N$ and from the term $DT_1^{(1)\dagger}$ is $-8.20 \times 10^{-22}emC_T \sigma_N$.

B. Cluster amplitudes and D_a

The calculated *normal* $T_1^{(1)}$ amplitudes are in excellent agreement with the corresponding CPHF mixing coefficients. Calculating the *normal* and the *pseudo* diagrams together, the D_a of atomic Hg is $-6.75 \times 10^{-22}em$. It is enhanced to $-6.92 \times 10^{-22}em$ when the two pseudo terms are calculated separately. A previous calculation [17] reported the CPHF D_a of atomic Hg as $-6.0 \times 10^{-22}em$. We attribute the difference of our result from the previous calculation to the inclusion of correlation effects in CC, beyond those present in CPHF, which are discussed in Section.IV. The different numerical methods used can also contribute to the discrepancy, however this would be small. The different results, when the *pseudo* terms are calculated together and separately with the *normal* terms, is the effect of the coupling between the two terms. Comparing the contributions from the *normal* and the *pseudo* diagrams, the *pseudo* diagrams though important, are just $\sim 9\%$ of the normal diagram contribution. The portion of the *pseudo* diagram contribution is however dependent on the size of the basis set. For example, with the basis $(1-14)s_{1/2}$, $(2-14)p_{1/2,3/2}$, $(3-$

$12)d_{3/2,5/2}$, $(4-8)f_{5/2,7/2}$ and $(5-9)g_{7/2,9/2}$, the contribution from the *pseudo* diagrams is 4%. This indicates that the contribution from the *pseudo* diagrams increases till it converge. The phase of the normal diagrams is determined by the phase of most dominant term, the Dirac-Fock contribution. For ^{199}Hg this is negative. On the other hand, the phase of the pseudo diagrams cannot be ascertained easily. Unlike the *normal* terms, the leading contribution from *pseudo* diagrams has $T_2^{(0)}$ which contributes to two terms $-H_{T-PT}T_2^{(0)}$ and $DT_2^{(0)}$. The phases of the dominant $H_{T-PT}T_2^{(0)}$ and $DT_2^{(0)}$ contributions determines the overall phase of the pseudo diagrams. That is, the relative phase of the normal and pseudo diagram is not a general trend. It depends on the phase of the of the dominant $T_2^{(0)}$ cluster amplitudes and hence it is atom specific.

VI. CONCLUSION

In this paper, We have numerically tested and demonstrated the inclusion of CPHF effects in coupled-cluster for atomic ^{199}Hg . We have shown that there are certain terms in the coupled-cluster theory for EDMs which are equivalent to the *normal* diagrams in the CPHF theory. This is demonstrated in the context of the EDM of ^{199}Hg arising from the T-PT electron-nucleus interaction, a property which is sensitive to the accuracy of the wavefunctions in the nuclear regions. The equivalence of the pseudo diagrams is more subtle and unlike *normal* cannot be shown explicitly. However, we identify the terms in coupled-cluster which correspond to the *pseudo* diagrams based on an analysis using many-body perturbation theory. The *pseudo* diagrams are the sum of two many-body perturbation theory diagrams [19]. Hence, in the coupled-cluster expression of D_a in Eq.(23), the direct and the conjugate terms when added give exactly the pseudo diagrams of CPHF. This shows that the coupled-cluster theory contains all the CPHF effects. The relative phases of the pseudo and the normal diagrams are atom-specific and hence cannot be generalized. An optimal basis consisting of 112 orbitals gives converged result and is in good agreement with the result of Martensson-Pendrill [17]. We have studied and analysed in detail the various many-body effects that play an important role in EDM of atomic Hg and impact of coupling between *normal* and *pseudo* diagrams.

Acknowledgments

We acknowledge Chiranjib Sur, Dmitry Budker and K.P. Geetha for discussions at various stages of the work.

[1] Lee T D and Yang C N, Brookhaven National Laboratory Report No. BNL 443-T91, 1957.

[2] Landau L D, Nucl.Phys., **3**, 127 (1957).

TABLE IV: Dominant contributions to D_a (in units of $10^{-21}C_{Tem\sigma_N}$) from the term $DT_2^{(0)}$.

Occ.	np	$DT_2^{(0)}$ (atomic units)		$D_a(\times 10^{-21}C_{Tem\sigma_N})$	
		<i>Direct</i>	<i>Exchange</i>	<i>Direct</i>	<i>Exchange</i>
$6s_{1/2}$	$6p_{1/2}$	0.0926	-1.077	-0.011	0.012
$6s_{1/2}$	$7p_{1/2}$	-0.238	0.269	-0.067	0.076
$6s_{1/2}$	$8p_{1/2}$	0.274	-0.287	-0.080	0.083
$6s_{1/2}$	$9p_{1/2}$	-0.248	0.209	-0.056	0.047
$6s_{1/2}$	$10p_{1/2}$	-0.108	0.056	-0.014	0.0071
$6s_{1/2}$	$11p_{1/2}$	-0.002	0.0009	-0.00013	0.000056
$6s_{1/2}$	$6p_{3/2}$	-0.088	0.0027	-0.0014	-0.000043
$6s_{1/2}$	$7p_{3/2}$	0.264	0.435	-0.011	-0.00018
$6s_{1/2}$	$8p_{3/2}$	0.362	-0.0057	-0.015	0.00023
$6s_{1/2}$	$9p_{3/2}$	-0.346	0.0324	-0.0061	0.00057
Total				-0.2597	0.226

- [3] Christensen J R, Cronin J W, Fitch V L and Turlay R, Phys. Rev. Lett., **13**, 138 (1964).
- [4] Aubert B et.al. (BABAR collaboration), Phys. Rev. Lett. **87**, 091801 (2001).
- [5] Abe K et.al. (BELLE collaboration), Phys. Rev. Lett. **87**, 091802 (2001).
- [6] Kobayashi M and Maskawa T, Prog. Theor. Phys., **49**, 652 (1973).
- [7] Commins E D, *Adv. At. Mol. and Opt. Phys.*, **40**, 1 (1999); Ginges J S M and Flambaum V V, Phys. Rep. **397**, 63 (2004); Maxim Pospelov and Adam Ritz, *Annals Phys.* **318**, 119 (2005).
- [8] Barr S M, *Int. Jour. Mod. Phys. A*, **8** (1993).
- [9] Sandars P G H, *J. Phys. B.* **1**, 511 (1968).
- [10] Romalis M V, Griffith W C, Jacobs J P and Fortson E N, Phys. Rev. Lett., **86**, 2505 (2001).
- [11] Rosenberry M A and Chupp T E, Phys. Rev. Lett. **86**, 22 (2001).
- [12] Ledbetter M P, Savukov I M, and Romalis M V, Phys. Rev. Lett. **94**, 060801 (2005).
- [13] Romalis M V and Ledbetter M P, Phys. Rev. Lett. **87**, 067601 (2001).
- [14] Takahashi Y et.al., *Proceedings of CP violation and it's origin*, edited by K. Hagiwara (KEK Reports, Tsukuba, 1997).
- [15] Takasu Y et.al., Phys. Rev. Lett. **91**, 040404 (2003).
- [16] Scielzo N D et.al., Phys.Rev.A, **73**, R010501 (2006).
- [17] Ann-Marie Maartensson-Pendrill, Phys. Rev. Lett, **54**, 1153 (1985).
- [18] Rossky P J and Karplus M, *J. Chem. Phys.* **73**, 6196 (1980); Caves T C and Karplus M, *J. Chem. Phys.* **50**, 3649 (1969).
- [19] Shukla A, Das B P, Andriessen J, Phys. Rev. A., **50**, 1155 (1994).
- [20] Bartlett R J, *Modern Electronic Structure Theory*, III, 1047, *edited by* D. R. Yarkony, published by
- [21] Liu Z W and Kelly H P, Phys. Rev. A., **45**, R4210 (1992).
- [22] Gopakumar G, et.al. (In preparation).
- [23] Cizek J, *Adv. Chem. Phys.*, **14**, 35 (1969).
- [24] Chaudhuri R K, Panda P K and Das B P, Phys. Rev. A. **59**, 1187 (1999).